SUPORTTING INFORMATION FOR

Ion coordination significantly enhancing photocatalytic activity of graphitic carbon nitride

Honglin Gao,[a,b] Shicheng Yan,*[a] Jiajia Wang,[a] and Zhigang Zou*[a,c]

[a] Eco-Materials and Renewable Energy Research Center (ERERC), College of Engineering and Applied Sciences, Nanjing University, Nanjing, Jiangsu 210093, P. R. China.

[b] Research Institute of Engineering and technology, Yunnan University, kunming, Yunnan 650091, P.R. China

[c] National Laboratory of Solid State Microstructures, School of Physics, Nanjing University, Nanjing, Jiangsu 210093, P. R. China

*To whom correspondence should be addressed. E-mail: yscfei@nju.edu.cn (S.Y.); zgzou@nju.edu.cn (Z.Z.)

Experimental procedures

Preparation of photocatalyst: The g-C_3N_4 was prepared by directly heating melamine in a semiclosed system to prevent sublimation of melamine. 10 g of melamine powder was put into an alumina crucible with a cover, and then heated to 500 ^oC in a muffle furnace for 2h at a heating rate of 10^oC/min; the further deammonation treatment was performed at 520 ^oC for 2h.

Characterization: Powder XRD measurements were performed on a Bruker D8 Advance diffractometer, using Cu *Kα* radiation (λ = 1.5406 Å), with 0.01^o 2θ steps from 5 to 60^o. Fourier transformed infrared (FTIR) spectra were recorded using a Nicolet Nexus 870 FTIR spectrometer. The UV-vis diffuse reflectance spectrum was recorded with a UV-2550 Ultraviolet-visible spectrophotometer at room temperature and transformed to the absorption spectrum according to the Kubelka–Munk relationship. The photoluminescence (PL) spectroscopy was obtained by using the Cary eclipse fluorescence spectrophotometer (USA). The Zeta potential of g-C_3N_4 particles in KCl solution with different concentration were determined by a zeta potential analyzer (Zeta PALS, Brookhaven Instruments Co., USA), the Refractive Index of Fluid is 1.330. The solid-state ^{13}C and ^{15}N NMR experiments were performed on a Bruker Advance III 400 spectrometer equipped with a 9.4 T magnet. The bulk conductivity was measured by a standard four probe method under a pressure of 28 MPa. The catalyst powders were pressed into a cylinder with a size of 11mm in diameter and 10.18mm in height.

Time-resolved fluorescence measurements were performed by using a time-correlated single photon counting (TCSPC) setup with a FM-4P-TCSPC spectrometer (Horiba Jobin Yvon, Paris, France). The excitation wavelength was 350 nm. Raw decay data presented as logarithm of photon counts versus time were analyzed with data analysis software of DAS6 (v6.6). The decay times were extracted by means of a reconvolution fit based on a triple exponential model. Considering that fluorescence intensity as a function of time gradually decays to the ground state, which process follows the multiexponential law of

$$I(t) = I_0 \sum_{i=1}^{n} a_i e^{-t/\tau_i},$$

where t is the decay time after the absorption, $I(t)$ is the fluorescence intensity at time t, I_0 is the intensity at time t= 0, τ_i is the lifetime and a_i is the pre-exponential factor, the intensity averaged-fluorescence lifetime $\overline{\tau}$ was calculated as

$$\overline{\tau} = \sum_{i=1}^{n} a_i \tau_i^2 \Big/ \sum_{i=1}^{n} a_i \tau_i \cdot$$

PL quantum efficiencies (φ) were determined with a Hamamatsu C9920 set-up, including an integrating sphere combined with a photonic multi-channel analyzer. The nonradiative decay rate (K_{nr}) was determined according to $K_{nr} = 1\text{-}\varphi/\overline{\tau}$.

Photocatalytic tests: The visible light induced catalytic H_2 evolution by the as-prepared g-C_3N_4 samples was carried out in a Pyrex top-irradiation reaction vessel connected to a closed glass gas-circulation system. The light irradiation system contains a 300W Xe lamp (Lamp House R300-3J, Japan) with cutoff filter L42 for visible light and a water filter to guarantee the light irradiation is purely visible light and eliminate the temperature effect. The average intensity of the focused irradiation to the system which detected using a photometer (Newport, 840-C) is 18.6 mW/cm^2. The transmission efficiency of L42 was detected by using UV-Vis transmission spectra (Varian, CARY 50probe). 0.1g catalyst was dispersed in an aqueous solution (100 mL) containing triethanolamine (10 vol.%) as the sacrificial electron donor and 0.5 Wt % Pt as the cocatalyst. Pt was photodeposited on the catalyst by using H_2PtCl_6 dissolved in the reaction solution. In the case of the addition of ions, the KCl, NaCl, $MgCl_2$ and Na_2SO_4 were respectively added with 0.1mol/L of concentration of cations in solutions. The system was evacuated several times to remove air prior to light irradiation. The evolved gases were analyzed by an online gas chromatography (GC-8A, Shimadzu) equipped with a thermal conductive detector, using argon as the carrier gas.

The above-mentioned setup for solar hydrogen production was also used for photodegradation of MO under visible light irradiation (300W Xe lamp, λ≥420nm). The photodegradation of MO was tested using 0.3 g of g-C_3N_4 as catalyst, which was dispersed in 100ml of MO solution (4mg/L). In the case of addition of ions, the KCl and Na_2SO_4 were respectively added with the 0.1mol/L of concentration of cations in solutions. The changes in MO concentration were monitored by using UV-Vis absorption spectra (Varian, CARY 50 probe, USA) to measure the remained MO. The degradation efficiency was determined by dividing C/C_0, where C is the remained MO concentration and C_0 is the starting MO concentration.

Table S1 Chemical composition of simulated seawater

Compound	Concentration, g/L
NaCl	24.53
$MgCl_2$	5.20
Na_2SO_4	4.09
$CaCl_2$	1.16
KCl	0.695
$NaHCO_3$	0.201
KBr	0.101
H_3BO_3	0.027
$SrCl_2$	0.025
NaF	0.003

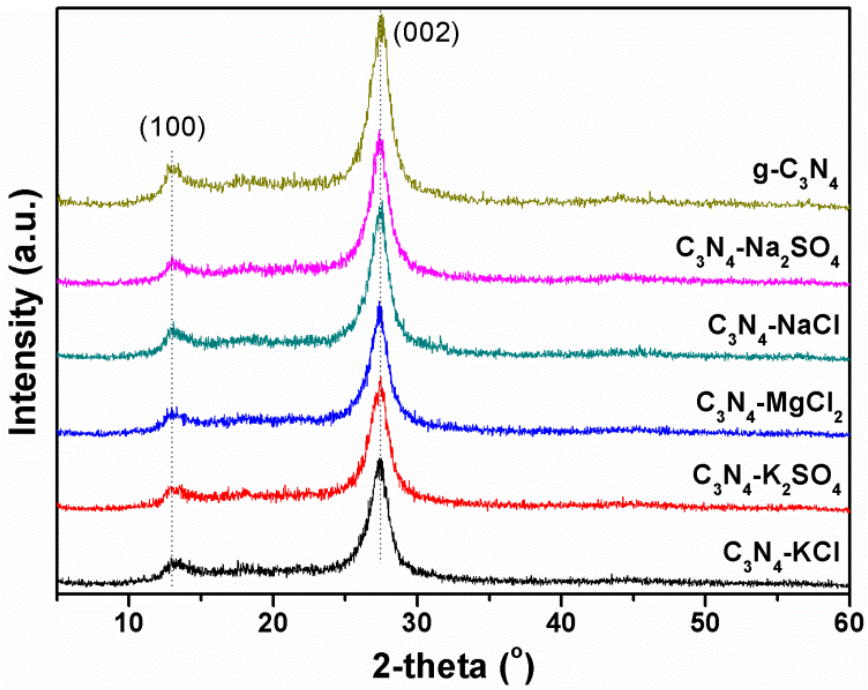

Figure S1 XRD patterns of g-C_3N_4 and C_3N_4-salt samples

In the X-ray diffraction patterns shown in Figure S1, we can see that two peaks are found in all the samples. It is widely accepted to that the g-C_3N_4 is based on tri-s-triazine building blocks. [1-3] The low-angle reflection peak at 12.95°, is indexed as (100), which corresponds to an in-planar repeat period of 6.86 nm in the crystal. The strongest XRD peak at 27.46° is a characteristic of interlayer stacking peak of aromatic systems of d=0.325 nm, indexed for graphitic materials as the (002) peak. The entire g-C_3N_4-salt samples exhibit the same peaks with bulk g-C_3N_4, indicating that the salt soaking treatment can not change the crystal structure of bulk g-C_3N_4.

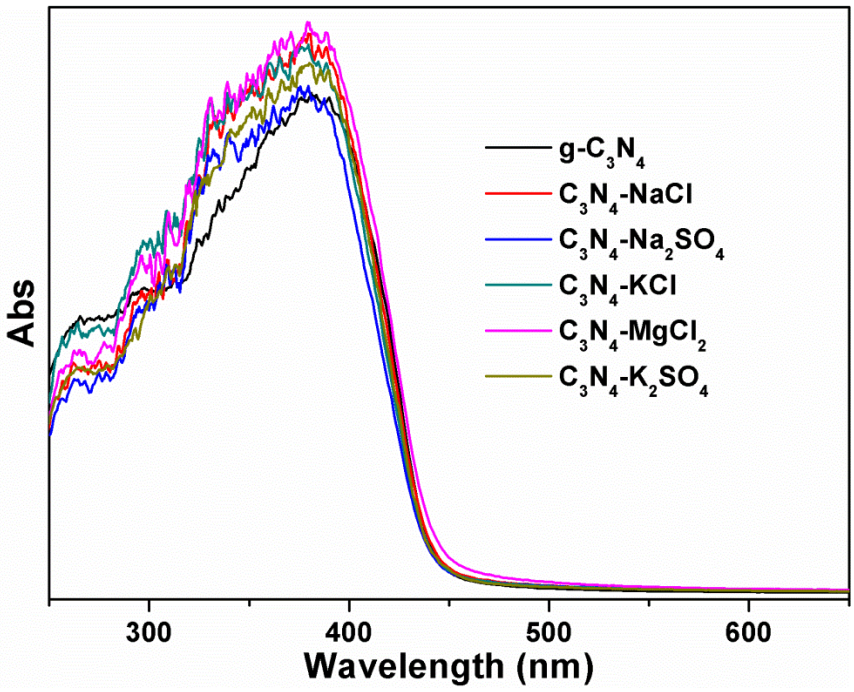

Figure S2 UV-Vis absorbance of g-C_3N_4 and C_3N_4-salt samples

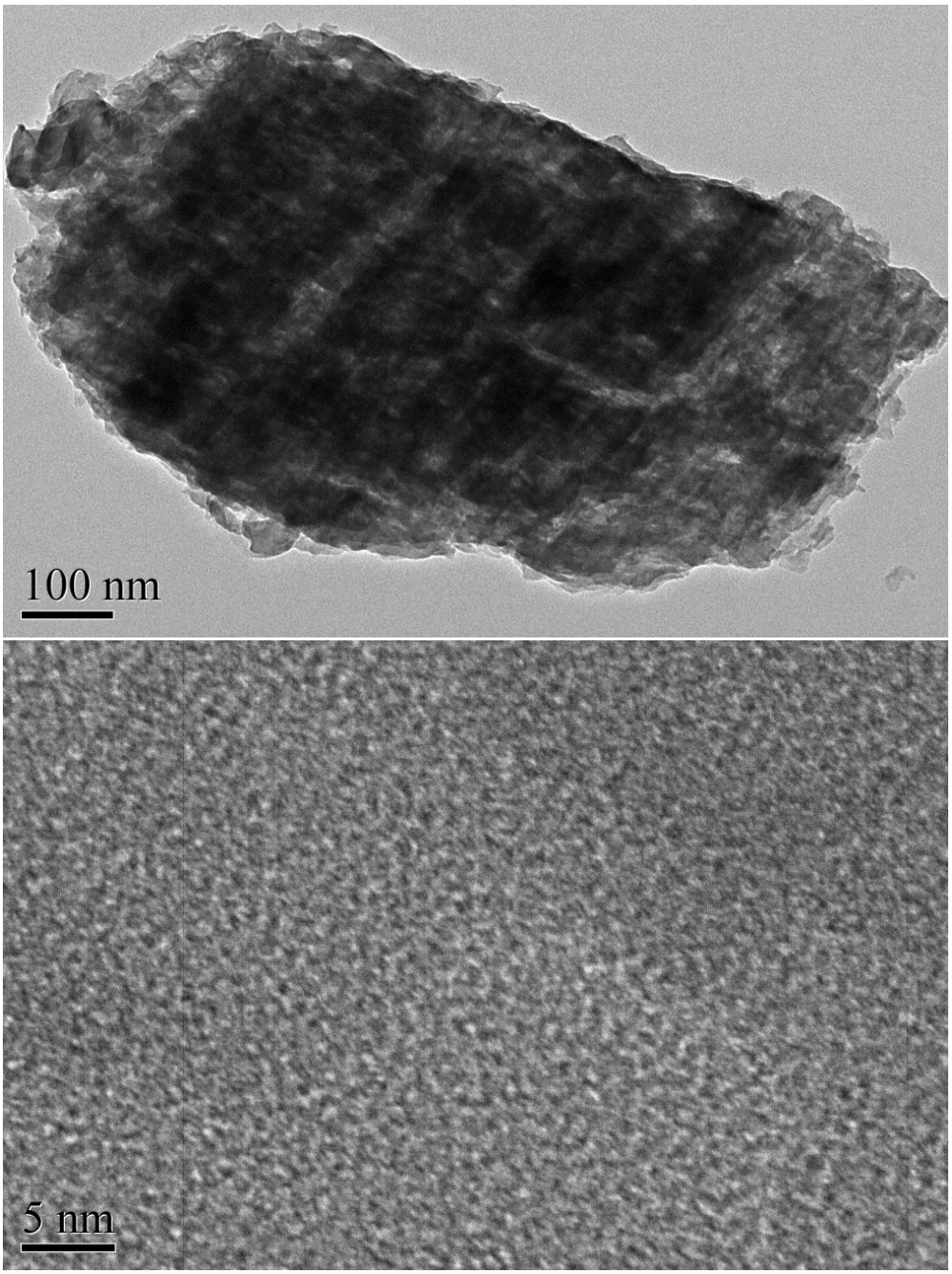

Figure S3 TEM (upper) and HRTEM (under) image of C_3N_4-KCl sample

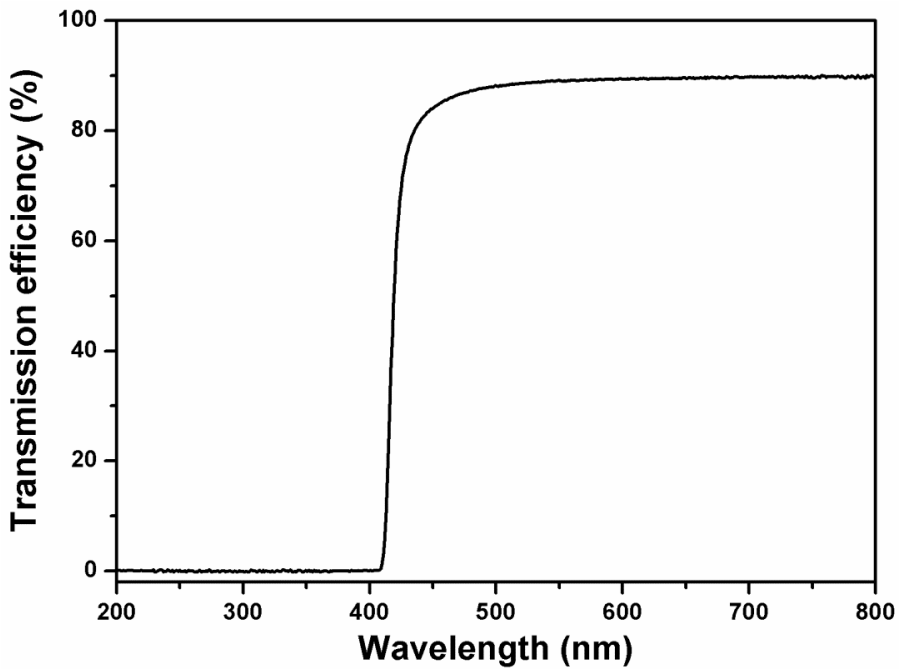

Figure S4 UV-Vis light transmission efficiency of the UV cut-off filter L42

References:

1. Thomas, A. Fischer, F. Goettmann, M. Antonietti, J. Müller, R. Schlögl, J. M. Carlsson, *J. Mater. Chem.* 2008, **18**, 4893-4908.

2. X. C. Wang, K. Maeda, A. Thomas, K. Takanabe, G. Xin, J. M. Carlsson, K. Domen and M. Antonietti, *Nat. Mater.* 2009, **8**, 76-80.

3. P. Niu, L. Zhang, G. Liu, H. M. Cheng, *Adv. Func. Mater.* 2012, **22**, 4763-4770

4. X. F. Li, J. Zhang, L. H. Shen, Y. M. Ma, W. W. Lei, Q. L. Cui, G. T. Zou, *Appl. Phys. A: Mater. Sci. Proc.* 2009, **94**, 387–392

5. W.J. Hsieh, P.S. Shih, J.H. Lin, C.C. Lin, U.S. Chen, S.C. Huang, Y.S. Chang, H.C. Shih, *Thin Solid Films*, 2004, **469-470**, 120-126